Article

Cell Reports

The *miR-17∼92* microRNA Cluster Is a Global Regulator of Tumor Metabolism

Graphical Abstract

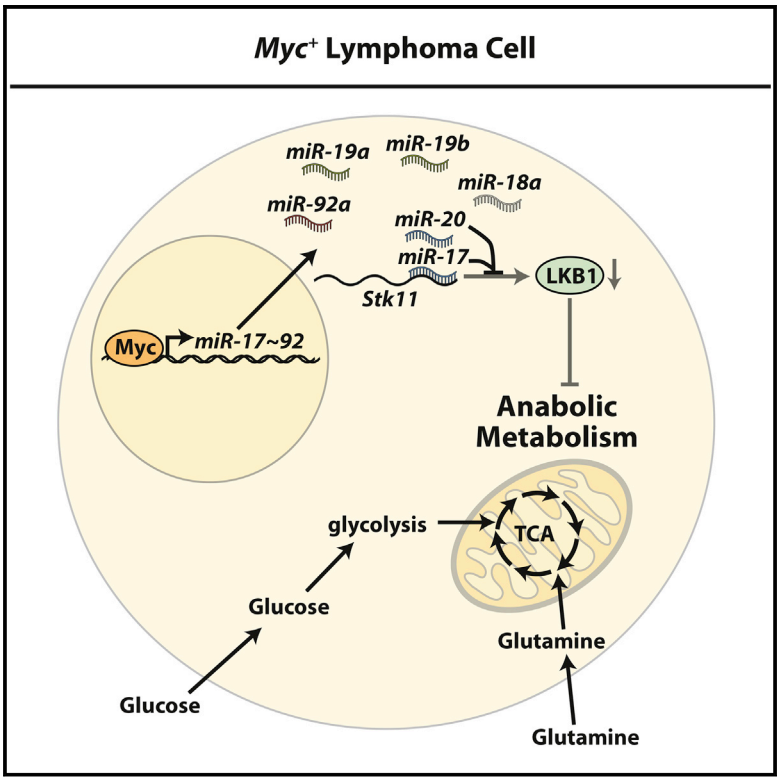

Highlights

- *miR-17∼92* is required for metabolic reprogramming of *Myc*$^+$ tumor cells
- *miR-17/20* is the primary metabolic regulatory element of *miR-17∼92*
- *miR-17* negatively regulates the tumor suppressor LKB1
- *miR-17*-dependent silencing of LKB1 dictates metabolic and tumorigenic potential

Authors

Said Izreig, Bozena Samborska, Radia M. Johnson, ..., Maxim N. Artyomov, Thomas F. Duchaine, Russell G. Jones

Correspondence

russell.jones@mcgill.ca

In Brief

Cancer cells re-wire cellular metabolic pathways to help fuel the increased bioenergetic and biosynthetic demands of malignant growth. Work by Izreig et al. demonstrate that this process is controlled in lymphoma cells by the *miR-17∼92* microRNA cluster, which coordinates tumor metabolism by silencing the LKB1 tumor suppressor pathway.

Accession Numbers

GSE77010

Izreig et al., 2016, Cell Reports *16*, 1915–1928
August 16, 2016
http://dx.doi.org/10.1016/j.celrep.2016.07.036

Cell Reports
Article

The *miR-17∼92* microRNA Cluster Is a Global Regulator of Tumor Metabolism

Said Izreig,[1,2] Bozena Samborska,[1,2] Radia M. Johnson,[1] Alexey Sergushichev,[3,4] Eric H. Ma,[1,2] Carine Lussier,[1,5] Ekaterina Loginicheva,[4] Ariel O. Donayo,[1,5] Maya C. Poffenberger,[1,2] Selena M. Sagan,[6] Emma E. Vincent,[1,2] Maxim N. Artyomov,[4] Thomas F. Duchaine,[1,5] and Russell G. Jones[1,2,*]

[1]Goodman Cancer Research Centre, McGill University, Montreal, QC H3A 1A3, Canada
[2]Department of Physiology, McGill University, Montreal, QC H3G 1Y6, Canada
[3]ITMO University, St. Petersburg 197101, Russia
[4]Department of Pathology and Immunology, Washington University in St. Louis, St. Louis, MO 63110, USA
[5]Department of Biochemistry, McGill University, Montreal, QC H3G 1Y6, Canada
[6]Department of Microbiology and Immunology, McGill University, Montreal, QC H3A 2B4, Canada
*Correspondence: russell.jones@mcgill.ca
http://dx.doi.org/10.1016/j.celrep.2016.07.036

SUMMARY

A central hallmark of cancer cells is the reprogramming of cellular metabolism to meet the bioenergetic and biosynthetic demands of malignant growth. Here, we report that the *miR-17∼92* microRNA (miRNA) cluster is an oncogenic driver of tumor metabolic reprogramming. Loss of *miR-17∼92* in *Myc*$^+$ tumor cells leads to a global decrease in tumor cell metabolism, affecting both glycolytic and mitochondrial metabolism, whereas increased *miR-17∼92* expression is sufficient to drive increased nutrient usage by tumor cells. We mapped the metabolic control element of *miR-17∼92* to the *miR-17* seed family, which influences cellular metabolism and mammalian target of rapamycin complex 1 (mTORC1) signaling through negative regulation of the LKB1 tumor suppressor. *miR-17*-dependent tuning of LKB1 levels regulates both the metabolic potential of *Myc*$^+$ lymphomas and tumor growth in vivo. Our results establish metabolic reprogramming as a central function of the oncogenic *miR-17∼92* miRNA cluster that drives the progression of MYC-dependent tumors.

INTRODUCTION

Tumor cells must manage their energetic resources to grow and survive. This involves coordinating metabolic activities to produce ATP, and the acquisition or synthesis of macromolecules (i.e., proteins, lipids, and nucleotides) at sufficient rates to meet the demands of malignant growth (Lunt and Vander Heiden, 2011). A common characteristic of cancer cells is the reprogramming of cellular metabolism to favor metabolic pathways that fuel aberrant cell growth such as aerobic glycolysis (i.e., the Warburg effect) and mitochondrial metabolism (Vander Heiden et al., 2009; Weinberg and Chandel, 2015). Many of the predominant oncogenic mutations observed in cancer also control tumor cell metabolism as part of their mode of action (Deberardinis et al., 2008; Jones and Thompson, 2009), linking metabolic dysregulation to tumor progression.

One of the major drivers of metabolic reprogramming in tumor cells is the c-Myc proto-oncogene (hereafter referred to as Myc), a transcription factor overexpressed or deregulated in over 50% of human cancers including hematopoietic, brain, breast, colorectal, and lung malignancies (Bredel et al., 2009; Cancer Genome Research Atlas, 2012, 2014; Li et al., 2013; Schmitz et al., 2012). Increased *MYC* expression is associated with poor prognosis in Burkitt Lymphoma (BL) (Lin et al., 2012b) and diffuse large B cell lymphoma (DLBCL) (Barrans et al., 2010; Savage et al., 2009; Zhou et al., 2014), with an overall 5-year survival rate of only ∼30% (Savage et al., 2009).

Myc promotes the re-wiring of tumor cell metabolism through the transcriptional regulation of metabolic pathway genes, including enzymes that regulate glycolysis, tricarboxylic acid (TCA) cycle metabolism, oxidative phosphorylation (OXPHOS), and mitochondrial biogenesis (Stine et al., 2015). Oncogenic Myc can also function as an amplifier of cellular gene expression programs (Lin et al., 2012a; Nie et al., 2012), which may occur through non-specific "invading" of enhancer and promoter regions, or recruitment of specific cofactors, such as Miz1 and Max, that help shape transcriptional responses triggered by supraphysiological levels of oncogenic Myc (Wolf et al., 2015). Myc also regulates the transcription of microRNAs (miRNAs), which are small, non-coding RNAs that negatively regulate mRNA stability and/or translation through partial complementary base pairing to the 3′ UTR of target mRNAs (Bartel, 2009). Myc has been associated with widespread repression of miRNA expression (Chang et al., 2008), but is also found to induce expression of the polycistronic miRNA cluster *miR-17∼92*. Originally identified as a candidate gene in the 13q31-q32 amplification observed in lymphoma (Ota et al., 2004), *miR-17∼92* is a direct transcriptional target of Myc (O'Donnell et al., 2005) and cooperates with Myc to promote lymphomagenesis in animal models (He et al., 2005). *miR-17∼92* expression is elevated in a number of human tumors, including cancers of the colon (He

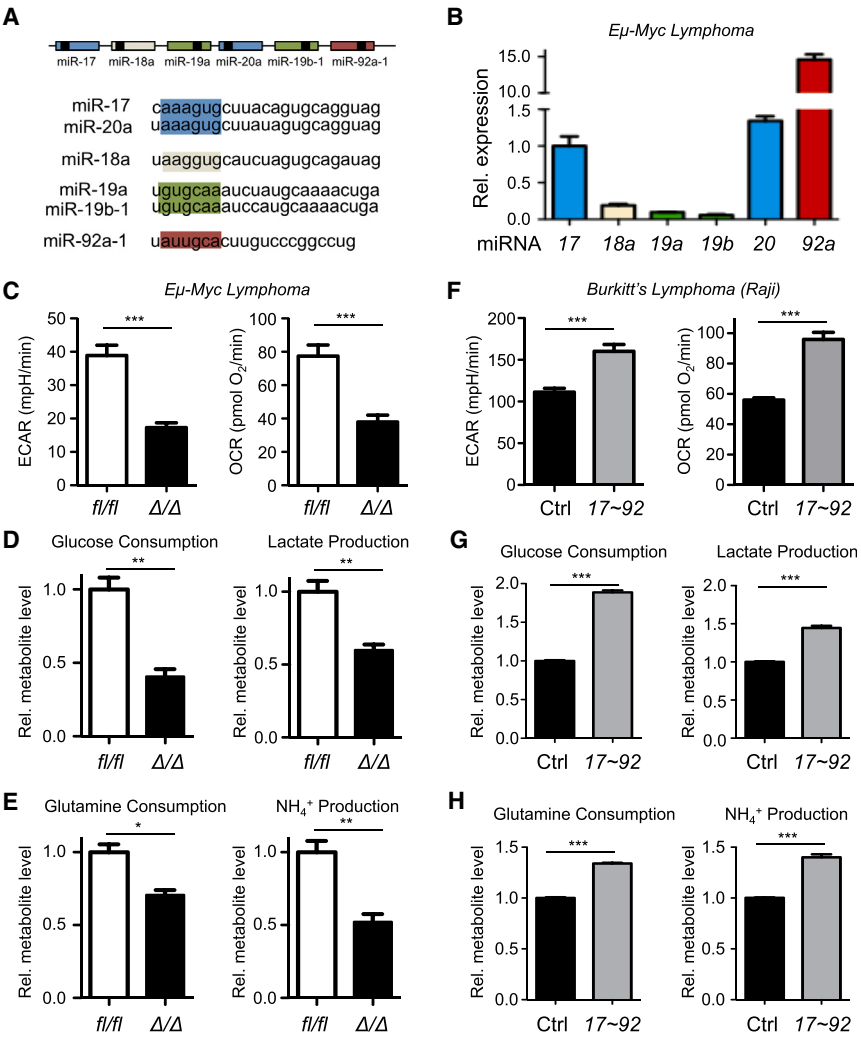

Figure 1. The Polycistronic miRNA Cluster *miR-17∼92* Regulates Glycoytic and Oxidative Metabolism in *Myc*$^+$ Lymphoma Cells

(A) Schematic of the *miR-17∼92* miRNA polycistron. Individual mature miRNAs with highlighted seed regions are listed, with seed families grouped by color.

(B) Relative expression of individual miRNAs of the *miR-17∼92* polycistron in Eμ-Myc lymphoma cells as determined by qPCR. Transcript levels were determined relative to U6 RNA and expressed relative to *miR-17* levels (set to 1).

(C) ECAR and OCR of Eμ-Myc lymphoma cells expressing (*fl/fl*) or lacking (*Δ/Δ*) *miR-17∼92*.

(D) Relative glucose consumption and lactate production by *fl/fl* and *Δ/Δ* Eμ-Myc lymphoma cells after 48 hr of culture.

(E) Relative glutamine consumption and ammonia production by lymphoma cells grown as in (D).

(F) ECAR and OCR of Raji cells ectopically expressing the entire *miR-17∼92* cluster (17∼92) or empty vector control (Ctrl).

(G) Relative glucose consumption and lactate production by Raji cells expressing control (Ctrl) or *miR-17∼92* expression (*17∼92*) vectors after 48 hr of culture.

(H) Relative glutamine consumption and ammonia production by Raji cells grown as in (G).

*p < 0.05; **p < 0.01; ***p < 0.001.

et al., 2005), lung (Hayashita et al., 2005), and DLBCL (Cerami et al., 2012; Olive et al., 2010; Pei et al., 2013).

Recent work indicated that elevated *miR-17∼92* expression can maintain tumor growth even when Myc is inactivated in tumors (Li et al., 2014), suggesting that *miR-17∼92* may mediate several of the pro-tumorigenic effects ascribed to Myc. Here, we describe an essential function for the Myc-regulated miRNA cluster *miR-17∼92* in mediating Myc-driven metabolic reprogramming, implicating control of tumor metabolism as a central part of *miR-17∼92* oncogenic activity.

RESULTS

miR-17-92 Regulates Glycolytic and Oxidative Metabolism in Lymphoma Cells

Myc has been characterized as a master regulator of tumor metabolism through the direct transcriptional regulation of metabolic enzymes involved in intermediary metabolism (Stine et al., 2015). However, Myc also induces the expression of *miR-17∼92*, a polycistronic miRNA cluster which encodes six individual miRNAs from a single RNA precursor (Figure 1A) (Olive et al., 2013). To investigate the influence of *miR-17∼92* on the metabolism of *Myc*$^+$ tumor cells, we used established Eμ-Myc B cell lymphomas harboring conditional floxed alleles of *miR-17∼92* (*miR-17∼92*$^{fl/fl}$, denoted hereafter as *fl/fl*) (Mu et al., 2009). Examination of miRNA expression revealed *miR-17*, *miR-20*, and *miR-92a* as the most abundant mature miRNAs of the cluster expressed in Eμ-Myc lymphoma cells (Figure 1B). Parental *fl/fl* Eμ-Myc lymphoma cells were cultured with 4-OHT to generate isogenic tumor cells with homozygous deletion of *miR-17∼92* (*miR-17∼92*$^{Δ/Δ}$, denoted as *Δ/Δ*) (Figures S1A and S1B). We did not observe compensation of mature miRNA expression from the paralogous clusters *miR-106a∼363* or *miR-106b∼25* in lymphoma cells lacking *miR-17∼92* (Figure S1C). Deletion of *miR-17∼92* led to a slight reduction in Eμ-Myc lymphoma cell proliferation as previously described (Mu et al., 2009) but did not significantly alter tumor cell viability (Figures S1D and S1E).

We next assessed the impact of *miR-17-92* deletion on the metabolism of *Myc*$^+$ lymphomas by measuring their extracellular acidification rate (ECAR), a measure of aerobic glycolysis, and oxygen consumption rate (OCR), a measure of OXPHOS (Wu et al., 2007). *Δ/Δ* lymphomas displayed an ∼50% reduction in both their ECAR and OCR compared to parental *fl/fl* lymphoma cells (Figure 1C). Consistent with the reduction in aerobic glycolysis, *Δ/Δ* lymphomas displayed lower glucose uptake and lactate production compared to lymphomas expressing

miR-17∼92 (Figure 1D). Glutamine consumption and ammonia production (a measure of glutaminolysis) were similarly reduced in *Δ/Δ* lymphoma cells (Figure 1E). The expression of key metabolic enzymes involved in glycolysis (Hk2, Aldolase, Ldha) and glutaminolysis (Gls1, Gls2) were reduced in *Δ/Δ* lymphoma cells compared to *fl/fl* controls (Figure S1F). Proliferating *Δ/Δ* lymphoma cells also displayed reduced cell size relative to parental tumor cells (Figure S1G).

miR-17∼92 cooperates with Myc to promote lymphomagenesis and tumor progression in animal models (He et al., 2005). To assess whether overexpression of *miR-17∼92* was sufficient to alter the metabolic activity of lymphoma cells, we ectopically expressed *miR-17∼92* in Raji cells (Figure S1H), a human BL cell line harboring a t(8;14)(q24;q32) *MYC-IGH* translocation (Hamlyn and Rabbitts, 1983). Ectopic expression of *miR-17∼92* increased the proliferative capacity but not the viability of Raji cells in culture (Figures S1I and S1J). In contrast to *miR-17∼92* deletion, ectopic expression of *miR-17∼92* increased both the ECAR and OCR of Raji cells (Figure 1F). We observed similar increases in both glucose consumption and lactate production (Figure 1G) and glutaminolysis (Figure 1H) in Raji cells overexpressing *miR-17∼92*. Together these data indicate that *miR-17∼92* is both sufficient to drive enhanced metabolism and required for global maintenance of glycolytic and oxidative metabolism in Myc-dependent lymphoma cells.

miR-17∼92 Is a Global Regulator of Myc-Dependent Metabolic Reprogramming

We next set out to identify pathways under *miR-17∼92* control by conducting RNA sequencing (RNA-seq) analysis of isogenic lymphoma cells expressing (*fl/fl*) or lacking (*Δ/Δ*) *miR-17∼92*. Deletion of *miR-17∼92* promoted widespread changes in gene expression in *Myc*$^{+}$ lymphoma, with the expression of >5,700 genes significantly altered in *Δ/Δ* lymphomas relative to control cells (Figure S2A; Table S1). Analysis of KEGG pathways significantly decreased in *Δ/Δ* lymphomas revealed enrichment in metabolic pathway genes, mRNA transport and translation, and proteasome and peroxisome pathway components (Figure 2A). Further analysis of the metabolic pathways genes influenced by *miR-17∼92* revealed a global decrease in metabolic pathways including glycolysis, the TCA cycle (Figure S2B), components of the electron transport chain (Figure S2C), amino acid metabolism, the pentose phosphate pathway, serine biosynthesis, and nucleotide biosynthesis (Figure 2A). We next assessed overlap between the *miR-17∼92*-regulated transcriptome and known Myc target genes (Kim et al., 2010). This analysis revealed that ∼45% of defined Myc target genes were significantly influenced by loss of *miR-17∼92* (Figure 2B). Enriched in this group of *miR-17∼92*-dependent Myc-target genes were metabolic pathway genes involved in central carbon metabolism and cellular biosynthesis (i.e., amino acid, purine, and pyrimidine biosynthesis). Details of differentially expressed *miR-17∼92*-dependent Myc-target genes are summarized in Figure S2D and Table S2.

We next assessed the impact of *miR-17∼92* loss on metabolic network connectivity in Myc-dependent lymphoma cells. This analysis, which is based on connectivity between metabolite abundance and metabolic enzyme gene expression (Jha et al., 2015; Vincent et al., 2015b), revealed several metabolic sub-networks dependent on *miR-17∼92* expression (Figure 2C). This network-based analysis confirmed a global downregulation of cellular metabolic pathways at the transcriptional level in *Δ/Δ* lymphomas. Pathways decreased in *miR-17∼92*-deficient Eμ-Myc lymphoma cells included glycolysis, and key branching pathways from the glycolytic pathway supporting nucleotide biosynthesis (i.e., pentose phosphate and serine biosynthesis pathways). The network also revealed lower TCA cycle metabolism and glutathione biosynthesis in *miR-17∼92*-deficient lymphomas, while highlighting increases in genes associated with inositol biosynthesis and acetate metabolism (*Acss1* and *Aldh3b1*). Taken together, these data suggest an active role for *miR-17∼92* in enforcing the Myc-dependent metabolic transcriptome.

Myc-Dependent Regulation of Central Carbon Metabolism Requires *miR-17∼92*

Given the decreased glycolytic and oxidative metabolism of *Myc*$^{+}$ lymphoma cells lacking *miR-17∼92* (Figure 1), we conducted stable isotope tracer analysis (SITA) on *fl/fl* and *Δ/Δ* Eμ-Myc lymphoma cells by culturing them with either U-[^{13}C]-glucose or -glutamine. *Δ/Δ* lymphoma cells displayed deceased overall abundance of intracellular metabolites involved in central carbon metabolism (Figure 3A). Total intracellular pyruvate and lactate levels were decreased by ∼50% in *Δ/Δ* Eμ-Myc cells (Figure 3A), due largely to reduced production of $^{13}C_3$-pyruvate and $^{13}C_3$-lactate isotopologues from glucose (Figure 3B). Similarly, the total abundance of TCA cycle metabolites including citrate and fumarate, as well as the incorporation of ^{13}C-glucose-derived carbon into these metabolite pools, were decreased in *Δ/Δ* cells relative to control lymphoma cells (Figures 3A and 3B). The synthesis of glutamate from α-ketoglutarate, which is mediated by glutamate dehydrogenase (GLDH) in Myc-driven cancer cells (Bott et al., 2015), was similarly decreased in *Myc*$^{+}$ lymphoma cells lacking *miR-17∼92* (Figure 3A). We observed a significant abundance of $^{13}C_3$ isotopologues of citrate, fumarate, and glutamate (blue bar, m+3), suggesting contribution of pyruvate carboxylase (PC) activity to TCA cycle anaplerosis in Eμ-Myc lymphoma cells (Figure 3B). Decreased mRNA levels for the glucose transporters Glut1 (*Slc2a1*) and Glut3 (*Slc2a3*) were observed in *Δ/Δ* Eμ-Myc cells (Figure S3), which may contribute to lower glucose utilization by these cells.

Myc is a major regulator of glutaminolysis (Gao et al., 2009; Wise et al., 2008) and regulates glutamine-dependent TCA cycle activity under basal and hypoxic conditions (Le et al., 2012). However, we found that *miR-17∼92* was required to support glutamine-dependent TCA cycle anaplerosis in Eμ-Myc lymphoma cells (Figure 3C). Incorporation of U-[^{13}C]-glutamine carbon into TCA intermediates was significantly reduced in *Δ/Δ* Eμ-Myc lymphoma cells, both in terms of total abundance (Figure 3C) and isotopomer distribution (Figure 3D). Of note, glutamine-dependent production of ^{13}C-citrate and ^{13}C-aspartate, which play essential roles in supporting cancer cell proliferation (Birsoy et al., 2015; Hatzivassiliou et al., 2005; Sullivan et al., 2015), were significantly reduced in *Δ/Δ* Eμ-Myc lymphoma cells.

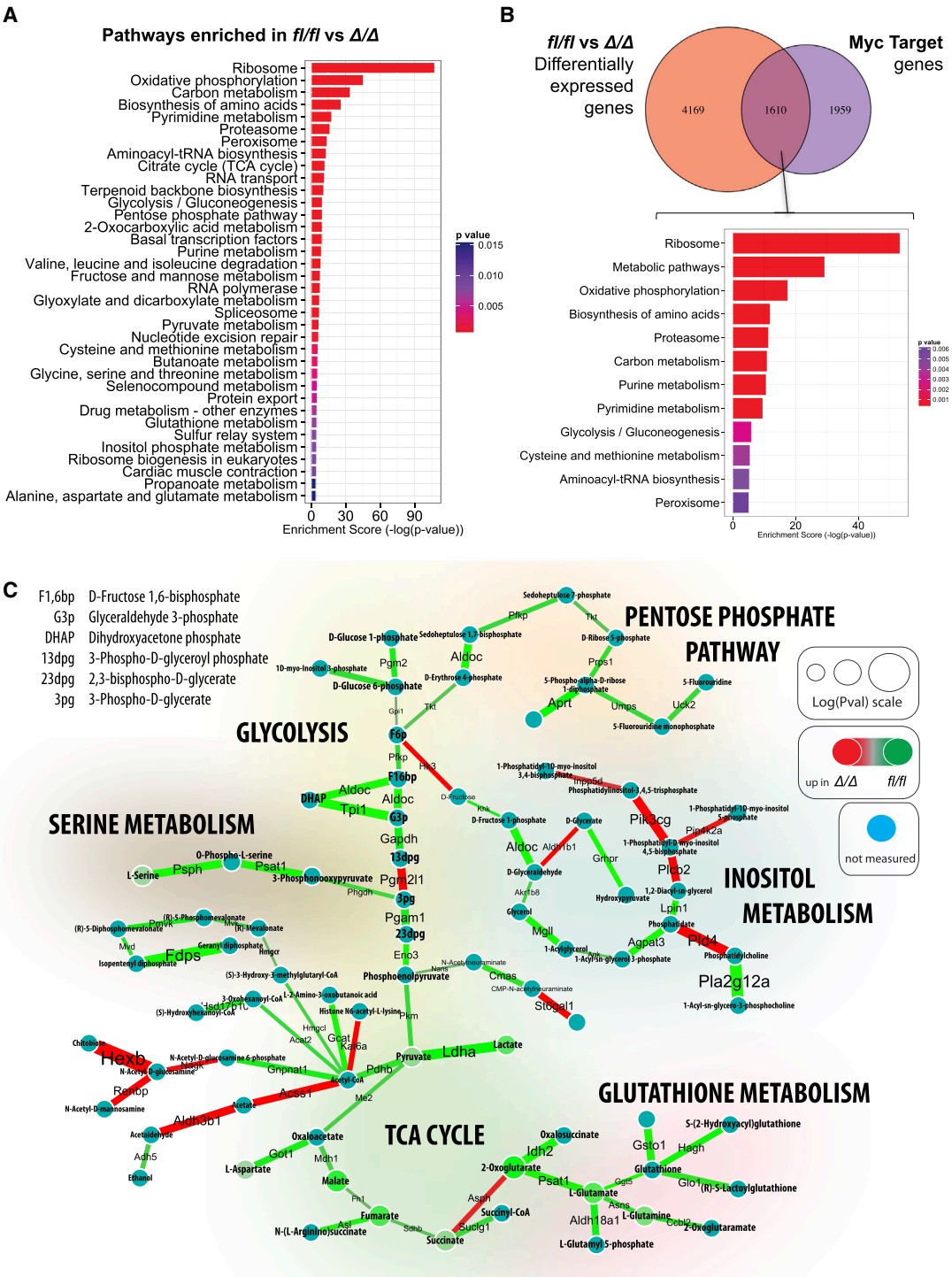

Figure 2. *miR-17∼92* Is a Global Regulator of Metabolism Downstream of Myc

(A) List of KEGG pathways significantly enriched in parental control (*fl/fl*) versus miR-17∼92-deficient (*Δ/Δ*) Eμ-Myc lymphoma cells (q value <0.1) using the Benjamini-Hochberg method.

(B) Analysis of Myc target genes differentially expressed in Eμ-Myc lymphoma cells lacking *miR-17∼92*. Top, Venn diagram depicting all differentially expressed genes enriched in *fl/fl* versus *Δ/Δ* Eμ-Myc lymphoma cells (5779) and overlap with Myc target genes (1610). Bottom, KEGG pathway analysis of *miR-17∼92*-dependent Myc target genes.

(legend continued on next page)

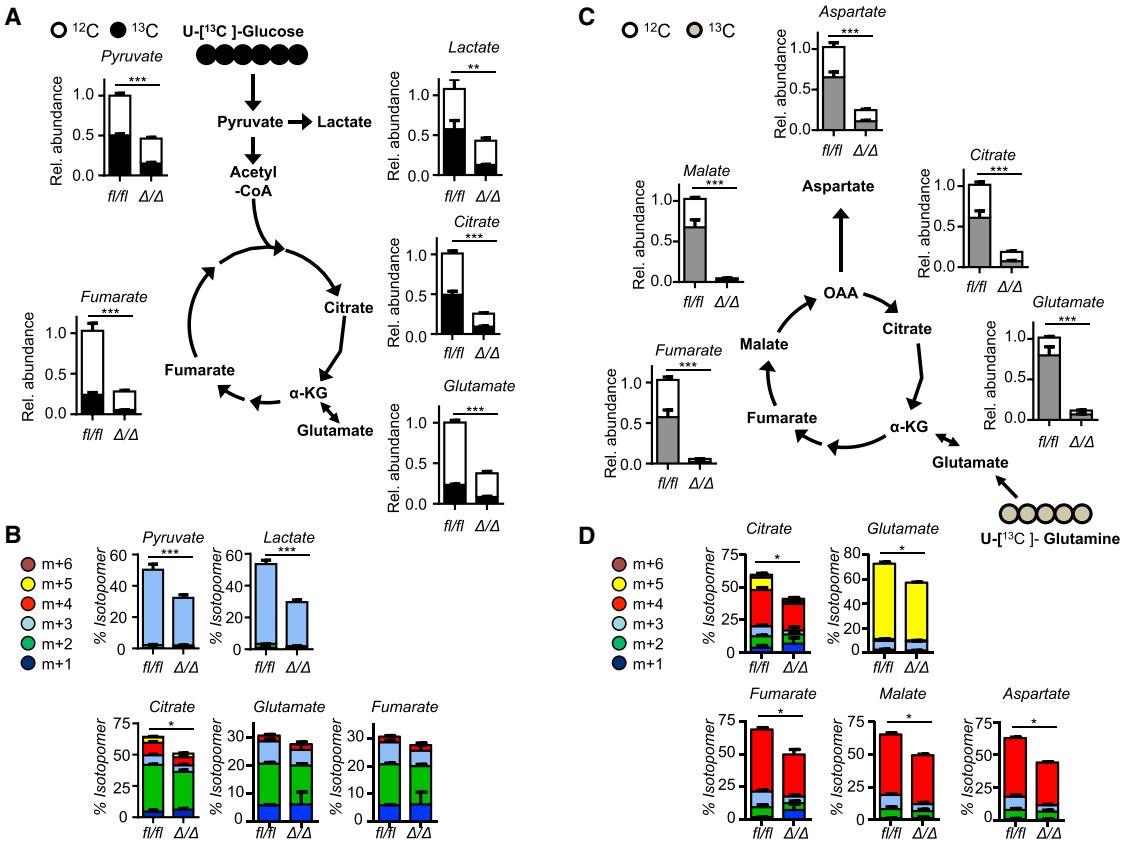

Figure 3. Regulation of Central Carbon Metabolism by *miR-17∼92*

(A) Relative abundance of U-[^{13}C]-glucose-derived metabolites from *fl/fl* and *Δ/Δ* Eμ-Myc lymphoma cells. Cells were cultured for 2 hr in medium containing U-[^{13}C]-glucose (25 mM) and unlabeled glutamine (2 mM), and the proportion of ^{13}C-labeled (black bar) or unlabeled (^{12}C, white bar) metabolites was determined by GC-MS. The height of the bar represents the total abundance of each metabolite, with the black bar representing the fraction of the metabolite pool derived from U-[^{13}C]-glucose.

(B) Mass isotopomer distribution (MID) of glycolytic intermediates (pyruvate, lactate), TCA cycle intermediates (citrate, fumarate), and glutamate for *fl/fl* and *Δ/Δ* Eμ-Myc lymphoma cells, cultured as in (A).

(C) Relative abundance of U-[^{13}C]-glutamine-derived metabolites from *fl/fl* and *Δ/Δ* Eμ-Myc lymphoma cells. Cells were cultured for 2 hr with U-[^{13}C]-glutamine (2 mM) and unlabeled glucose (25 mM), and the proportion of ^{13}C-labeled (gray bar) or unlabeled (^{12}C, white bar) metabolites determined by GC-MS.

(D) MID of U-[^{13}C]-glutamine-derived metabolites in *fl/fl* and *Δ/Δ* Eμ-Myc lymphoma cells, cultured as in (C).

*p < 0.05; **p < 0.01; ***p < 0.001.

miR-17 and *-20* Drive Metabolic Reprogramming Downstream of Myc

Given that the *miR-17∼92* gene encodes six mature miRNAs comprising four seed families (Figure 1A), we next sought to determine which miRNAs contribute to the metabolic regulatory activity of the cluster. We engineered a series of *miR-17∼92*-deficient Eμ-Myc lymphoma cell lines re-expressing the full miRNA cluster (*+17∼92*) or mutant *miR-17∼92* alleles lacking specific seed family members (Figure 4A). The relative expression of each mature miRNA in control (*fl/fl*) and *miR-17∼92* mutant cell lines was verified by qPCR (Figure S4A). Seahorse analysis of these lymphoma cell lines revealed differential contributions of each *miR-17∼92* seed family to the bioenergetic profiles of Eμ-Myc lymphoma cells (Figure 4B). Addback of the full *miR-17∼92* cluster rescued the OCR and enhanced the ECAR of *Δ/Δ* cells, confirming our earlier results that elevated *miR-17∼92* expression can enhance glycolysis (Figures 1F and 1G). Addback of the cluster lacking only *miR-92a* (Δ92) or *miR-19a* and *miR-19b* (Δ19a,b) increased both OCR and ECAR above levels seen in *fl/fl* cells, whereas addback of a mutant *miR-17∼92* allele lacking the *miR-17* family members *miR-17* and *miR-20a* (*Δ17,20*) failed to rescue the ECAR and OCR of *Δ/Δ* cells (Figure 4B).

Further metabolic profiling was conducted using individual *Δ/Δ* lymphoma cell clones expressing all components of

(C) Integrated metabolic network analysis for *fl/fl* versus *Δ/Δ* Eμ-Myc lymphoma cells. The direction and magnitude of fold changes in enzyme expression or metabolite abundance between conditions is indicated on a green (enriched in *fl/fl*) to red (enriched in *Δ/Δ*) color scale. Enzymes are represented by connecting lines between metabolites, with the color of the edge indicating the fold change and the thickness reflecting the significance of differential expression. Round nodes represent metabolites, with the differential abundance of each metabolite indicated by the size of the node.

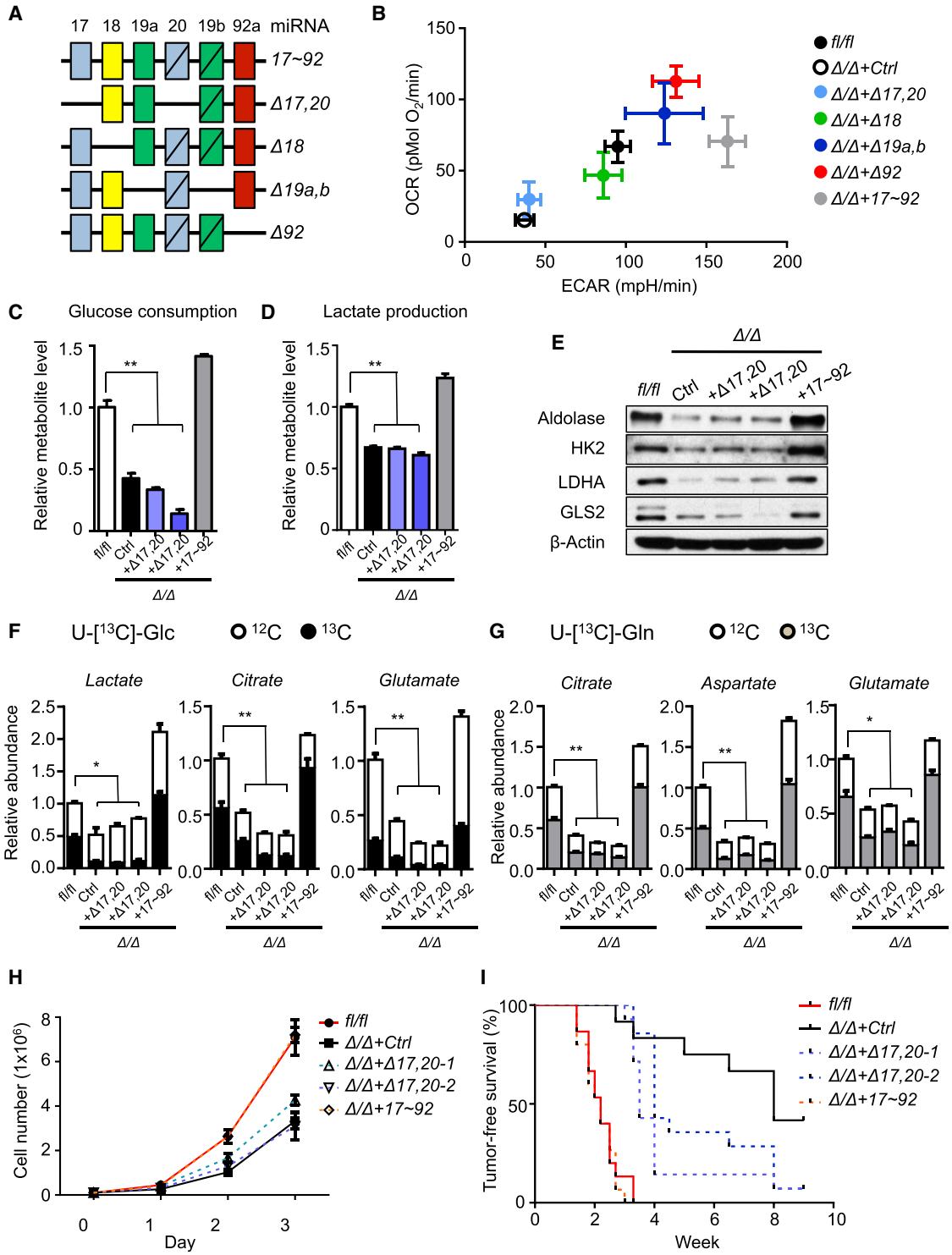

Figure 4. The *miR-17* Family Members *miR-17* and *miR-20a* Are Required for *miR-17∼92*-Dependent Metabolic Reprograming

(A) Schematic of *miR-17∼92* constructs lacking individual seed families used in this study.

(B) OCR versus ECAR plot for *fl/fl* and *Δ/Δ* Eμ-Myc lymphoma cells, as well as *Δ/Δ* lymphomas expressing *miR-17∼92* addback constructs described in (A).

(C and D) Relative glucose consumption (C) and lactate production (D) of control (*fl/fl*, white bar), *miR-17∼92*-deficient (*Δ/Δ*, black bar), or *miR-17/20*-deficient (*+Δ17/20*, blue bars) Eμ-Myc lymphoma cells after 48 hr of culture. *Δ/Δ* lymphoma cells re-expressing the entire *miR-17∼92* polycistron (*+17∼92*, gray bar) are included.

(E) Immunoblot of metabolic enzyme expression from lysates of Eμ-Myc lymphoma cells described in (B). Actin levels are shown as a control for protein loading. HK2, hexokinase-2; LDHA, lactate dehydrogenase A; GLS2, glutaminase-2.

(legend continued on next page)

miR-17∼92 except *miR-17* and *miR-20a* (*Δ17,20*). Lymphoma cells lacking *miR-17/20* displayed similar reductions in glucose consumption (Figure 4C), lactate production (Figure 4D), glutamine consumption (Figure S4B), and ammonia production (Figure S4C) compared to *Δ/Δ* lymphoma cells, which was fully rescued only through addback of the full *miR-17∼92* cluster. The reduction in glycolysis and glutaminolysis correlated with reduced levels of key glycolysis (Hk2, Aldolase, Ldha) and glutaminolysis (Gls2) enzymes in *Δ17,20* lymphoma cells relative to control cells (either *fl/fl* or full *miR-17∼92* addback) (Figure 4E).

We next used SITA to assess whether the *miR-17* seed family influences nutrient utilization by *Myc*$^{+}$ lymphoma cells. Control (*fl/fl*), *miR-17∼92*-deficient (*Δ/Δ*), *miR-17∼92* addback, or *Δ17,20* lymphoma cells were cultured in medium containing either U-[^{13}C]-glucose or -glutamine, and metabolite abundances determined by gas chromatography-mass spectrometry (GC-MS). Re-expression of *miR-17∼92* was sufficient to restore both glucose- and glutamine-dependent metabolic flux in *Δ/Δ* lymphoma cells (Figures 4F, 4G, and S4D–S4G). Ectopic *miR-17∼92* expression actually enhanced metabolic flux in *Δ/Δ* lymphoma cells beyond control levels, marked by increased production of lactate from ^{13}C-glucose (Figure 4F) and TCA cycle metabolites from ^{13}C-glutamine (Figures 4G and S4G). In contrast, *Δ17,20* lymphoma cells displayed similar ^{13}C-labeling patterns to *Δ/Δ* lymphoma cells (Figures 4F and 4G).

Finally, we assessed the contribution of *miR-17/20* to the tumorigenic potential of Eμ-Myc lymphomas. While re-expression of full-length *miR-17∼92* restored the proliferative capacity of *Δ/Δ* lymphoma cells to control levels, *Δ17,20* failed to rescue lymphoma cell proliferation in vitro (Figure 4H). Next, we injected nude mice with control (*fl/fl*) or *miR-17∼92*-deficient Eμ-Myc lymphoma cells expressing full-length *miR-17∼92 or Δ17,20*, and monitored palpable tumor formation over time. While *control* lymphomas and *Δ/Δ* lymphomas re-expressing *miR-17∼92* formed tumors rapidly (median onset of ∼2 weeks), the development of tumors lacking *miR-17* and *-20* (*Δ17,20*) was significantly slower, with an average latency of 4 weeks (Figure 4I). For one clone in particular (*Δ17,20-2*), >30% of animals remained tumor-free for up to 8 weeks, compared to 50% for animals who had received *Δ/Δ* lymphoma cells (Figure 4I).

LKB1 Is a Direct Target of the *miR-17* Seed Family

miRNAs act to repress mRNA translation or promote mRNA degradation via partial complementary binding to the 3′ UTR of target mRNAs (Fabian et al., 2010). Previous work has linked deregulated *miR-19* expression to the lipid phosphatase Pten (Mu et al., 2009; Olive et al., 2009), which may affect glycolysis through modulation of PI3K-Akt signaling. However, Pten protein levels were unaffected by loss of *miR-17∼92* in *Δ/Δ* lymphoma cells (Figure S5A), and lymphoma cells lacking *miR-19* did not display major changes in ECAR or OCR (Figure 4B).

We used the miRNA prediction algorithm Targetscan (Agarwal et al., 2015) and curated miRNA-mRNA interactions (Helwak et al., 2013) to identify *Stk11*, which encodes the serine-threonine kinase Liver Kinase B1 (LKB1), as a putative *miR-17* family target. Previous work had identified LKB1 as a potential target of *miR-17* in ovarian cancer cells (Liu et al., 2015). The seed region of *miR-17/20* was predicted to bind to one site (base pairs 122–130) in the mouse *Stk11* 3′ UTR sequence (Figure 5A), and that this 3′ UTR target site was retained across several mammalian species including humans (Figure S5B). This was intriguing given that haploinsufficiency of LKB1, rather than biallelic inactivation of the gene, is commonly associated with tumor development (Vaahtomeri and Mäkelä, 2011). LKB1 is also a negative regular of tumor metabolism whose loss promotes the Warburg effect in tumors (Faubert et al., 2014; Shackelford et al., 2009). We conducted 3′-rapid amplification of cDNA end (RACE) using mRNA isolated from Eμ-Myc lymphoma cells and, consistent with previous reports (Smith et al., 1999), found that *Stk11* possesses an alternative poly-adenylation sequence that gives rise to both short and long 3′ UTR isoforms (denoted S1 and L1, for short and long, respectively) that contain the *miR-17/20* targeting sequence (Figure S5C).

We next assessed whether *miR-17* directly acts on the 3′ UTR of *Stk11* mRNA to regulate its expression. We first used a reporter assay in which the *Stk11* 3′ UTR was cloned downstream of a luciferase reporter gene to assess miRNA-dependent suppression of the 3′ UTR sequence. Normalized luciferase activity was reduced in 293T cells expressing either the S1 or L1 form of the *Stk11* 3′ UTR (Figure S5D), indicating suppression of this 3′ UTR by endogenous miRNAs or other RNA binding proteins. The *Stk11* 3′ UTRs were suppressed further by ectopic expression of *miR-17* (Figure 5B). Mutating the complementary *miR-17* target site (Figure 5A) abolished *miR-17*-dependent regulation of the *Stk11* 3′ UTR in this assay (Figures 5B and S5D).

We next expressed FLAG-tagged versions of LKB1 in 293T cells using expression constructs encoding *Stk11* mRNA with no 3′ UTR (Δ), wild-type 3′ UTR (WT), or a mutated 3′ UTR lacking complementarity with the *miR-17* seed region (MUT) (Figure S5E). Protein levels of FLAG-LKB1 were reduced in cells expressing the wild-type *Stk11* 3′ UTR when co-transfected with a *miR-17* expression vector (Figure 5C). Conversely, FLAG-LKB1 with the mutant *Stk11* 3′ UTR was refractory to *miR-17* expression (Figure 5C).

(F) Relative abundance of U-[^{13}C]-glucose-derived metabolites in *fl/fl*, *Δ/Δ*, *miR-17/20*-deficient (*+Δ17/20*), and *miR-17∼92*-expressing (*+17∼92*) Eμ-Myc lymphoma cells. Cells were cultured for 2 hr with U-[^{13}C]-glucose, and the proportion of ^{13}C-labeled (black bar) or unlabeled (^{12}C, white bar) metabolites was determined by GC-MS.

(G) Relative abundance of U-[^{13}C]-glutamine-derived metabolites in Eμ-Myc lymphoma cells described in (F). Cells were cultured for 2 hr with U-[^{13}C]-glutamine, and the proportion of ^{13}C-labeled (gray bar) or unlabeled (^{12}C, white bar) metabolites was determined by GC-MS.

(H) Growth curves of control (*fl/fl*), *miR-17∼92*-deficient (*Δ/Δ+Ctrl*), *miR-17/20*-deficient (*Δ/Δ+Δ17/20*), and *miR-17∼92*-expressing (*Δ/Δ+17∼92*) Eμ-Myc lymphoma cells.

(I) Kaplan-Meier curve showing latency to tumor onset for Eμ-Myc lymphoma cells described in (H). The number of mice analyzed per genotype was as follows: *fl/fl*, n = 15; *Δ/Δ+Ctrl*, n = 12; *Δ/Δ+Δ17/20-1*, n = 14; *Δ/Δ +Δ17/20-2*, n = 14; and *Δ/Δ+17∼92*, n = 15.

*p < 0.05; **p < 0.01.

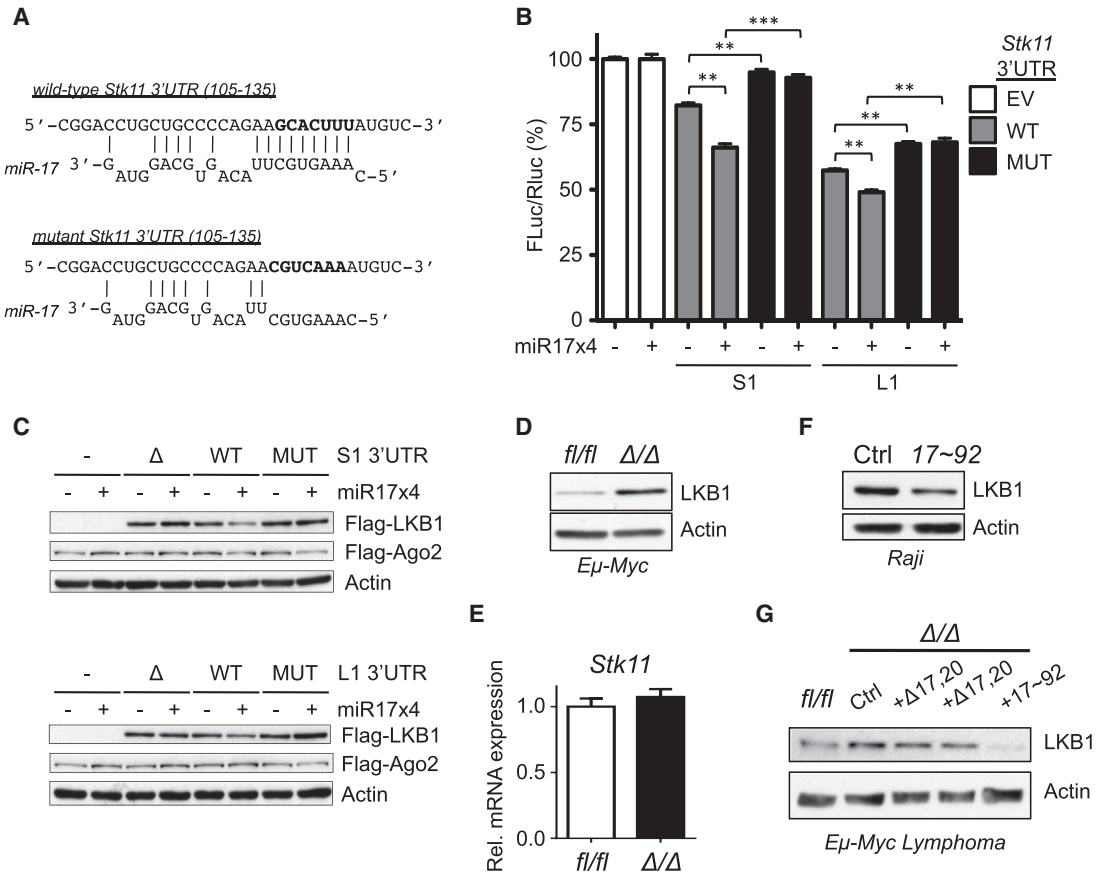

Figure 5. The Tumor Suppressor LKB1 Is a Target of *miR-17*

(A) Alignment of *miR-17* and the wild-type (WT) 3′ UTR of mouse *Stk11*. The putative recognition site for the *miR-17* seed family in the *Stk11* 3′ UTR is shown in boldface. The sequence of the mutant (MUT) *Stk11* 3′ UTR used in subsequent experiments is shown.

(B) 293T cells expressing FLAG-Ago2 (293T-Ago2) were transfected with empty vector (EV) or luciferase reporter constructs for the short (S1) or long (L1) variants of the mouse *Stk11* 3′ UTR containing either the wild-type (WT) or mutated (MUT) *miR-17* family recognition site as in (A). Cells were co-transfected with (+) or without (–) a *miR-17x4* expression plasmid. Shown is the mean ± SEM for the FLuc/RLuc ratio for triplicate samples, normalized to control cells (EV).

(C) Immunoblot of FLAG-LKB1 protein expression in 293T-Ago2 cells co-transfected with (+) or without (–) a *miR-17x4* expression plasmid and FLAG-LKB1 expression plasmids lacking the 3′ UTR (Δ), or containing the WT or MUT 3′ UTR sequence fused to the *Stk11* CDS. Shown are protein levels for FLAG-LKB1 and FLAG-Ago2 for the S1 (top) and L1 (bottom) *Stk11* 3′ UTR isoforms.

(D) Immunoblot for LKB1 expression in *fl/fl* and *Δ/Δ* Eμ-Myc lymphoma cells.

(E) Relative expression of *Stk11* mRNA in *fl/fl* and *Δ/Δ* Eμ-Myc lymphoma cells.

(F) Immunoblot for LKB1 expression in Raji cells expressing control vector (Ctrl) or ectopic expression of *miR-17∼92* (17∼92).

(G) Immunoblot for LKB1 expression in *miR-17/20*-deficient Eμ-Myc lymphoma cells (+*Δ17/20*).

**p < 0.01; ***p < 0.001.

We next examined the impact of *miR-17/20* on LKB1 expression in lymphoma cells. LKB1 protein levels were elevated in *Δ/Δ* Eμ-Myc lymphoma cells compared to control cells (Figure 5D). *Stk11* mRNA levels were unaffected by deletion of *miR-17∼92* (Figure 5E), suggesting a mechanism of translational suppression of LKB1 mRNA by *miR-17*. In contrast, LKB1 protein levels were reduced in Raji cells ectopically expressing *miR-17∼92* (Figure 5F). Lymphoma cells lacking *miR-17* and *-20* expression (*Δ17,20*) displayed elevated LKB1 expression similar to *miR-17∼92*-deficient lymphomas, whereas addback of the entire *miR-17∼92* cluster potently reduced LKB1 protein levels in Eμ-Myc lymphoma cells (Figure 5G).

miR-17∼92 Regulates mTORC1 Signaling in Lymphoma through LKB1 Silencing

LKB1 is a tumor suppressor mutated in a number of human cancers and plays a central regulatory role in tumor metabolic and cell growth control through downstream effects on AMPK and mTOR signaling (Shackelford and Shaw, 2009). One prediction of our findings was that *miR-17∼92* may influence these pathways through suppression of LKB1-dependent signaling. Deletion of *miR-17∼92* promoted an increase in basal AMPK signaling, as determined by increased AMPKα phosphorylation at Thr-172 and increased phosphorylation of the AMPK targets ULK1 (Ser-555) and Raptor (Ser-792) in *Δ/Δ* lymphoma cells (Figure 6A). mTORC1 pathway activity, as determined by rS6

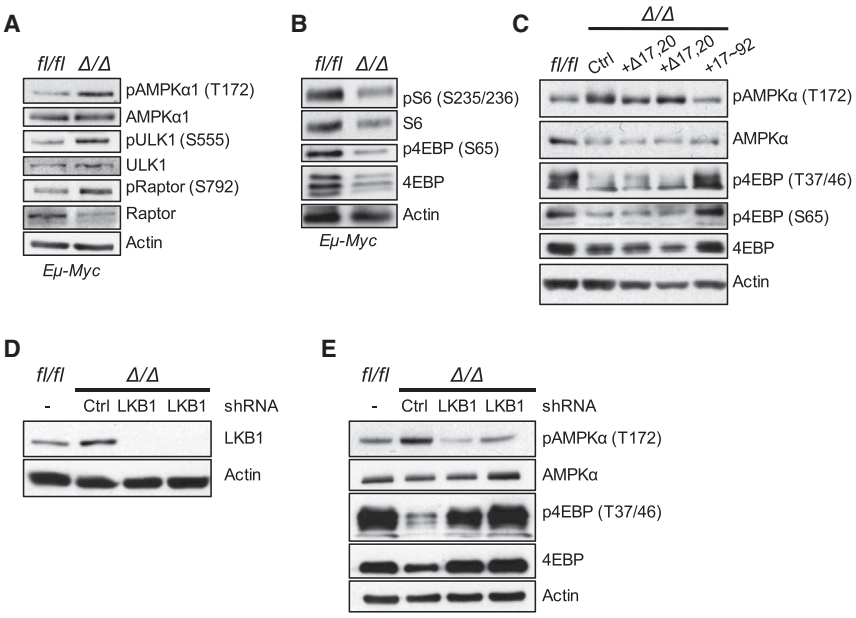

Figure 6. *miR-17~92* Regulates AMPK and mTORC1 Activity through LKB1

(A) Immunoblot for AMPK (total and phospho-T172), ULK (total and phospho-S555), and Raptor (total and phospho-S792) protein levels in *fl/fl* and *Δ/Δ* Eμ-Myc lymphoma cells.

(B) Immunoblot of mTORC1 pathway activation targets in *fl/fl* and *Δ/Δ* Eμ-Myc lymphoma cells. Shown are protein levels for rS6 (total and phospho-S235/236) and 4E-BP1 (total and phospho-S65), with actin levels assessed as a loading control.

(C) Immunoblot for AMPK and mTORC1 activation in *miR-17/20*-deficient Eμ-Myc lymphoma cells (+*Δ17/20*) cultured as in (A).

(D) Immunoblot of LKB1 protein levels in control (*fl/fl*), or *miR-17~92*-deficient (*Δ/Δ*) Eμ-Myc lymphoma cells expressing control (Ctrl) or LKB1-specific shRNAs (LKB1).

(E) Immunoblot of AMPK and mTORC1 pathway activation in control (*fl/fl*) or *Δ/Δ* Eμ-Myc lymphoma cells expressing control (Ctrl) or LKB1-specific shRNAs (LKB1) as in (D). Shown are protein levels for AMPK (total and phospho-T172) and 4E-BP1 (total and phospho-T37/46).

and 4EBP phosphorylation, was decreased in *Δ/Δ* lymphoma cells (Figure 6B). Similar patterns of increased AMPK activity and decreased mTORC1 activity were observed in lymphoma cells specifically lacking *miR-17* and *-20* (*Δ17/20*, Figure 6C), implicating the *miR-17* seed family as a mediator of these signaling changes. Reducing LKB1 levels in *Δ/Δ* lymphoma cells by stable short hairpin RNA (shRNA) expression (Figure 6D) reversed the effects of *miR-17~92* deletion on AMPK and mTORC1 pathway activity (Figure 6E).

LKB1 Suppression by *miR-17* Dictates Metabolic Reprogramming and Tumorigenic Potential of *Myc*$^+$ Lymphomas

We next examined the contribution of *miR-17/20*-dependent suppression of LKB1 to the metabolic reprogramming that drives *Myc*$^+$ lymphoma growth. Silencing LKB1 increased metabolic enzyme expression in *Δ/Δ* lymphoma cells compared to *Δ/Δ* cells transduced with a control shRNA hairpin (Figure 7A). The recovery of metabolic gene expression in LKB1 shRNA-expressing *Δ/Δ* lymphoma cells correlated with increased ECAR and OCR levels (Figure 7B), increased glucose consumption and lactate production (Figure S6A), and increased glutaminolysis (Figure S6B) in these cells. We next cultured *Δ/Δ* lymphoma cells expressing control or LKB1 shRNAs with either U-[^{13}C]-glucose (Figures 7C and S6C) or U-[^{13}C]-glutamine (Figures 7D and S6D). Silencing LKB1 in *Δ/Δ* lymphomas restored the defects in central carbon metabolism normally seen in these cells and was characterized by a re-emergence of Warburg metabolism (^{13}C-glucose to lactate conversion, Figure 7C) and increased contribution of both glucose and glutamine to the TCA cycle (Figures 7C, 7D, S6C, and S6D).

Finally, we examined whether silencing LKB1 was sufficient to rescue the tumorigenic potential of lymphoma cells lacking *miR-17~92*. Expression of shRNAs targeting LKB1 reversed the proliferative defect of *Δ/Δ* lymphoma cells in vitro (Figure 7E). When injected into nude mice, *Δ/Δ* lymphoma cells expressing LKB1 shRNA (Δ/Δ+shLKB1) formed palpable lymph node tumors with latency similar to wild-type Eμ-Myc lymphomas expressing *miR-17~92* (*fl/fl*) (Figure 7F), despite the fact that these cells lacked expression of any mature *miR-17~92*-derived miRNAs. These data indicate that the effects of *miR-17~92* loss on cell metabolism and tumor growth can be overcome simply by disrupting LKB1 signaling, highlighting the *miR-17*-LKB1 circuit as a key regulator of tumor metabolism and growth.

DISCUSSION

Myc is among the most implicated genes in human cancer (Zack et al., 2013) and has been shown to coordinate multiple cellular behaviors in support of malignancy (Dang, 2012). Here, we describe a new paradigm for Myc-dependent metabolic reprogramming involving the polycistronic miRNA *miR-17~92*. Using isogenic Myc-dependent lymphoma cells lacking *miR-17~92*, we demonstrate that *miR-17~92* is a critical regulator of metabolic reprogramming in *Myc*$^+$ tumors. We show that *miR-17~92* is required to sustain both glycolytic and oxidative metabolism and promote multiple anabolic pathways required for tumor growth, while amplified *miR-17~92* expression, which is observed in many tumor types, is sufficient for cell autonomous upregulation of tumor metabolic activity. Our data implicate the *miR-17* seed family (comprising *miR-17* and *miR-20*) as the key regulatory element of *miR-17~92* that influences both metabolic reprogramming and the oncogenic potential of Myc-dependent lymphomas through negative regulation of the LKB1 tumor suppressor. Our results establish metabolic reprogramming as a central function for *miR-17~92* and implicate metabolic control as an essential part of the oncogenic activity of this miRNA cluster.

Previous work has established *miR-17~92* as an oncogenic miRNA cluster through its ability to promote tumor cell

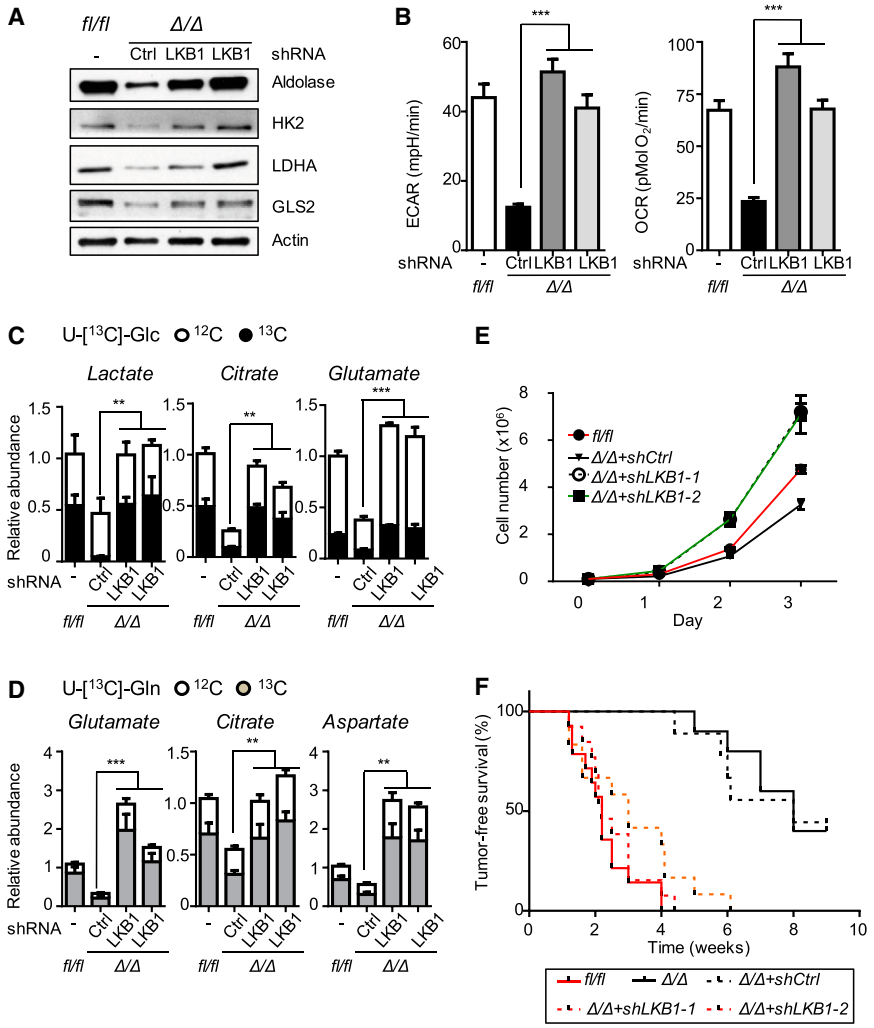

Figure 7. *miR-17/20*-Dependent Control of LKB1 Dictates Metabolic and Tumorigenic Potential of *Myc*$^+$ Lymphoma

(A) Immunoblot for metabolic enzyme expression in control (*fl/fl*) or *Δ/Δ* Eμ-Myc lymphoma cells expressing control (Ctrl) or LKB1-specific shRNAs (LKB1).

(B) ECAR and OCR of control (*fl/fl*, white) or *Δ/Δ* Eμ-Myc lymphoma cells expressing control (Ctrl, black) or LKB1-specific shRNAs (LKB1) as in (A). Shown are two independent LKB1 shRNA clones (dark gray, *shLKB1*-1; light gray, *shLKB1*-2).

(C) Relative abundance of lactate, citrate, and glutamate in control (*fl/fl*) or *Δ/Δ* Eμ-Myc lymphoma cells expressing the indicated shRNAs. Cells were cultured for 2 hr in medium containing U-[^{13}C]-glucose and unlabeled glutamine, and the proportion of ^{13}C-labeled (black bar) or unlabeled (^{12}C, white bar) metabolites as determined by GC-MS is shown.

(D) Relative abundance of glutamate, citrate, and aspartate in *Δ/Δ* Eμ-Myc lymphoma cells cultured with U-[^{13}C]-glutamine. The proportion of ^{13}C-labeled (gray bar) or unlabeled (^{12}C, white bar) metabolites is shown.

(E) Growth curve of *fl/fl* (red) or *Δ/Δ* Eμ-Myc lymphoma cells expressing control (Ctrl, black) or LKB1-specific shRNAs (shLKB1-1, dashed line; shLKB1-2, green).

(F) Kaplan-Meier curve showing latency to tumor onset for control (*fl/fl*, n = 14) and *miR-17∼92*-deficient Eμ-Myc lymphoma cells (*Δ/Δ*, n = 9), or *Δ/Δ* lymphomas expressing control (Ctrl, n = 10) or LKB1-specific (LKB1-1, n = 13; LKB1-2, n = 12) shRNAs.

**p < 0.01; ***p < 0.001.

proliferation, cell viability, and angiogenesis while inhibiting cellular differentiation and senescence (Dews et al., 2006; Olive et al., 2010, 2013). Our data extend the regulatory repertoire of *miR-17∼92* to include many of the core metabolic processes in cancer. Although Myc can influence specific metabolic nodes such as glutaminolysis through suppression of miRNAs targeting metabolic enzymes (Gao et al., 2009), our data indicate that *miR-17∼92* functions broadly to support Myc-dependent metabolic programs. Loss of *miR-17∼92* in *Eμ-Myc* lymphoma cells leads to reduced transcription of core bioenergetic pathway genes (glycolysis; TCA cycle; OXPHOS) while simultaneously altering anabolic pathways (pentose phosphate pathway; biosynthesis of serine, aspartate, and glutamine; purine and pyrimidine metabolism) and ribosome biogenesis. This global reduction in metabolic pathway gene expression is coupled to reduced nutrient consumption and processing, including glucose and glutamine, which serve as two major carbon sources for lymphoma growth.

Although *miR-17∼92* cooperates with Myc to promote tumor aggressiveness (He et al., 2005; Mu et al., 2009; Olive et al., 2009), recent work has demonstrated Myc-independent roles for *miR-17∼92* in tumor maintenance (Li et al., 2014). Our data indicate that *miR-17∼92* expression influences almost 50% of the Myc-regulated transcriptome in *Myc*$^+$ lymphomas. Included in this regulation are a majority of metabolic pathway genes previously established as Myc targets (Lin et al., 2012a; Wang et al., 2011), suggesting that many of the effects on metabolic reprogramming ascribed to Myc route through *miR-17∼92*. These observations counter the argument that the reduced metabolism of *miR-17∼92*-deficient (*Δ/Δ*) and *miR-17/20*-deficient (*Δ17,20*) lymphoma cells is simply a by-product of reduced cell size and/or proliferation but rather reflects the action of the cluster on global metabolic gene expression. Given the broad effect of *miR-17∼92* loss on metabolic gene expression, it is unlikely that *miR-17∼92* directly regulates these genes through direct miRNA:mRNA pairing. We speculate that *miR-17∼92* functions to reinforce Myc-dependent metabolic reprogramming indirectly by broadly regulating the expression of transcription factors (or other regulators) involved in metabolic reprogramming.

Processing of primary *miR-17∼92* (*pri-miR-17∼92*) transcripts results in differential expression of mature miRNA species in tissues (Du et al., 2015), with *miR-17*, *-20*, and *-92* being the most abundant mature miRNAs produced from the *miR-17∼92* cluster in the lymphoma cells tested. Evidence shows that *miR-17* is often the most expressed miRNA of the cluster in tumors

(Knudsen et al., 2015; Yu et al., 2010). Lymphoma cells lacking *miR-17* and *-20* (*Δ17,20*) display increased LKB1 expression, decreased mTORC1 activity, and deficiencies in glycolytic and oxidative metabolism identical to tumor cells lacking *miR-17∼92*. Beyond its role in cancer, *miR-17∼92* plays important roles in other biological processes including hematopoietic cell development, stem cell renewal, and axial patterning (Olive et al., 2013). Based on our data, we hypothesize that metabolic regulation is a central function of *miR-17* family miRNAs under both normal and pathological conditions.

Our finding that LKB1 is repressed by *miR-17* family miRNAs establishes a regulatory link between oncogenic Myc signaling and the LKB1 tumor suppressor pathway. LKB1 has wide-ranging impact on tumor growth and metabolism, in part by modulating AMPK and mTORC1 activity (Shackelford and Shaw, 2009). Reduced LKB1 signaling promotes the development of tumors with high mTORC1 activity and an aggressive metabolic phenotype (Dupuy et al., 2013; Faubert et al., 2014; Shaw et al., 2004). Somatic inactivating mutations in LKB1 are observed in many cancers, including ∼30% of non-small cell lung cancer (NSCLC) cases (Gill et al., 2011). However, biallelic loss of LKB1 is rare among tumors with inactivating LKB1 mutations. Rather, haploinsufficiency of LKB1, similar to other tumor suppressors including *Tsc2, Pten*, and *Smad4*, is sufficient to promote tumorigenesis (Yoo et al., 2002), arguing that gene dosage is critical for LKB1-dependent tumor suppression. In this regard, *miR-17∼92*-dependent post-transcriptional regulation of LKB1 may help fine-tune its tumor suppressor functions. This has clear implications for the tumorigenic potential of Myc^+ tumors, as silencing LKB1 reverses the severe metabolic and growth defects of lymphoma cells lacking *miR-17∼92*.

Our results indicate that post-transcriptional regulation of LKB1 by miRNAs can allow tumor cells to bypass LKB1-mediated growth suppression without the need for inactivating *STK11* mutations. This raises the possibility that miRNA-dependent tuning of LKB1 levels may be a general mechanism for balancing cellular bioenergetics and cell growth in cancer, and may contribute to the pathophysiology of LKB1-regulated diseases such as Peutz-Jeghers syndrome. It is possible that endogenous miRNAs in addition to *miR-17* are capable of silencing LKB1 in tumor cells and that miRNAs targeting other components of the LKB1 complex, such as *miR-451* (Godlewski et al., 2010), may exert similar effects on tumor metabolism by influencing LKB1-dependent signaling. *miR-17* and *-20* belong to a larger miRNA family that includes *miR-93, -106a,* and *-106b*, all sharing a common seed sequence (5′-AAA GUG-3′). Interestingly, *miR-106a* and *-106b*, which are also encoded by miRNA clusters (*miR-106a∼363* and *miR-106b∼25*, respectively), are also associated with oncogenesis (Conkrite et al., 2011; Landais et al., 2007), although our data suggest that these miRNAs do not compensate for the loss of *miR-17∼92* in the lymphoma cells examined here. Whether related miR-17 family members also influence LKB1 expression and/or tumor metabolism remains to be determined. Together our data highlight a central role for *miR-17∼92* in balancing both metabolic advantage and growth potential in cancer.

EXPERIMENTAL PROCEDURES

Cell Lines, DNA Constructs, and Cell Culture

The generation of Eμ-Myc *Cre-ERT2*$^+$;*miR-17∼92*$^{fl/fl}$ lymphoma cells has been described previously (Mu et al., 2009). Eμ-Myc cells were cultured on a layer of irradiated *Ink4a*-null MEF feeder cells in DMEM and IMDM medium (50:50 mix) supplemented with 10% fetal bovine serum (FBS), 2 mM glutamine, and β-mercaptoethanol. Raji cells were cultured in RPMI medium supplemented with 10% FBS and 2 mM glutamine. Retroviral-mediated gene transfer into lymphoma cells was conducted as previously described (Faubert et al., 2013).

For growth assays, cells were seeded at a density of 1×10^5 cells/ml in 3.5-cm dishes, and cell counts were determined via trypan blue exclusion using a TC20 Automated Cell Counter (Bio-Rad). For viability measurements, cells were stained with Fixable Viability Dye eFluor 780 (eBioscience) and analyzed using a Gallios flow cytometer (Beckman Coulter) and FlowJo software (Tree Star). Cell size was determined by forward scatter using flow cytometry.

Seahorse Analysis and Metabolic Assays

OCR and ECAR were determined using an XF96 Extracellular Flux Analyzer (Seahorse Bioscience) using established protocols (Faubert et al., 2014; Vincent et al., 2015a). For media metabolite determination, cells were cultured for 2 days, and culture medium was analyzed for extracellular metabolites (glucose, glutamine, lactate, and ammonia) using a BioProfile Analyzer (NOVA Biomedical) as previously described (Vincent et al., 2015a). Metabolic parameters were assessed in lymphoma cells undergoing logarithmic growth and standardized to cell number.

For metabolomics experiments using ^{13}C-labeled glucose or glutamine, lymphoma cells (3–5 × 10^6 per 3.5-cm dish) were cultured for 2 hr in glucose- and glutamine-free DMEM/IMDM (50:50 mix) containing 10% dialysed FBS (Wisent Bio Products) and either uniformly labeled [^{13}C]-glucose or [^{13}C]-glutamine (Cambridge Isotope Laboratories). ^{12}C-glutamine (2 mM) or -glucose (25 mM) were added back to the culture medium depending on the tracer used. Cells were washed twice with saline and then lysed in ice-cold 80% methanol, sonicated, derivatized as tert-butyldimethylsilyl (TBDMS) esters, and analyzed by GC-MS using previously described protocols (Dupuy et al., 2013; Faubert et al., 2014; McGuirk et al., 2013). Metabolite abundance was expressed relative to an internal standard (D-myristic acid) and normalized to cell number. Additional experimental details are described in Supplemental Experimental Procedures.

Immunoblotting, Quantitative Real-Time PCR, and RNA Sequencing

Lymphoma cell lines were subjected to SDS-PAGE and immunoblotting using CHAPS and AMPK lysis buffers as previously described (Faubert et al., 2013). Primary antibodies against hexokinase 2, aldolase, LDHA, GLS2, β-actin, 4EBP (total, phospho-T36/47, and phospho-S65), rS6 (total and phospho-S235/236), ULK (total and phosphor-S555), Raptor (total and phospho-S792), AMPKα (total and phospho-T172), and FLAG-tag were obtained from Cell Signaling Technology. Primary antibody against LKB1 (Ley 37D/G6) was from Santa Cruz Biotechnology.

For qPCR quantification of mature miRNAs, Qiazol was used isolate RNA, miRNEasy Mini kit was used to purify miRNAs and total mRNA, and cDNA synthesized using the miScript II RT kit (QIAGEN). qPCR was performed using the SensiFAST SYBR Hi-ROX kit (Bioline) and an AriaMX Real Time Pcr system (Agilent Technologies). miScript primer assays (QIAGEN) were used to detect mature miRNAs of the *miR-17∼92* cluster, with miRNA expression normalized relative to U6 RNA levels. RNA preparation and library construction for RNA sequencing was conducted as previously described (Jha et al., 2015). Libraries were sequenced using a HiSeq 2500 (Illumina) using 40 bp by 10 bp pair-end sequencing. Gene set enrichment analysis (GSEA) on RNA-seq data was conducted using the gage function and non-parametric Kolmogorov-Smirnov test from the GAGE R Bioconductor package (Luo et al., 2009). Network integration of RNA-seq and metabolite datasets was conducted as previously described (Jha et al., 2015). Additional experimental details are described in Supplemental Experimental Procedures.

3′ UTR Cloning and Validation

3′ UTR isoforms for mouse *Stk11* were determined by 3′ RACE as previously described (Wu et al., 2010). GeneArt DNA fragments (Life Technologies) for

either the wild-type *Stk11* 3′ UTR or harboring a mutated *miR-17* seed region (bases 2–8 in the seed region) were cloned into the XhoI/XbaI sites of the pmirGLO vector (Promega). 293T cells (10^5 cells/well) stably expressing FLAG-Ago2 (Valdmanis et al., 2012) were transfected with individual pmirGLO-3′ UTR constructs with or without co-transfection of a *miR-17* expression plasmid (*miR-17x4*) (Hong et al., 2010). Cells were lysed 48 hr post-transfection, and the ratio of luciferase to renilla luciferase activity determined using a Dual-Glo Luciferase assay kit (Promega) and a FLUOstar Omega plate reader. FLAG-tagged LKB1 expression constructs were generated by PCR amplification of the full-length LKB1 coding sequence from Eμ-Myc lymphoma RNA, using sequence specific primers to amplify inserts with short or long forms of the *Stk11* 3′ UTR.

Tumor Xenograft Assays

Lymphoma cells were resuspended in Hank's balanced salt solution (HBSS) and injected intravenously (10^6 cells/mouse in 200 μl) into CD-1 nude mice (Charles River Laboratories). Tumor onset was monitored by palpation of inguinal and axillary lymph nodes, and tumor-free survival scored as the time elapsed between injection and first detection of palpable tumors as previously described (Faubert et al., 2013). All procedures were carried out in accordance with guidelines of the Canadian Council on Animal Care, as approved by the Animal Care Committee of McGill University.

Statistical Analysis

Statistics were determined using paired Student's t test, ANOVA, or log-rank (Mantel-Cox) using Prism software (GraphPad) unless otherwise stated. Data are calculated as the mean ± SEM for biological triplicates and the mean ± SD for technical replicates unless otherwise stated. Statistical significance is represented in figures by *$p < 0.05$; **$p < 0.01$; ***$p < 0.001$; ****$p < 0.0001$.

ACCESSION NUMBERS

The accession number for the RNA-seq data reported in this paper is GEO: GSE77010.

SUPPLEMENTAL INFORMATION

Supplemental Information includes Supplemental Experimental Procedures, six figures, and two tables and can be found with this article online at http://dx.doi.org/10.1016/j.celrep.2016.07.036.

AUTHOR CONTRIBUTIONS

Experimental design was conducted by S.I., B.S., S.M.S., T.F.D., and R.G.J., and the majority of experiments were executed by S.I. and B.S. Data interpretation was performed by S.I., B.S., E.H.M., T.F.D., and R.G.J. RNA-seq and metabolic network analysis were conducted by R.M.J., A.S., and M.N.A. The manuscript was written and edited by S.I., B.S., E.E.V., T.F.D., and R.G.J.

ACKNOWLEDGMENTS

We thank members of R.G.J.'s laboratory for discussion of the manuscript, and Drs. Andrea Ventura, Ping Mu, Jerry Pelletier, Nathalie Johnson, and Peiqing Sun for their gift of reagents. We acknowledge technical assistance from the McGill/GCRC Metabolomics and Flow Cytometry core facilities, and the Centre for Applied Genomics at the Hospital for Sick Children. The GCRC Metabolomics Core Facility is supported by grants from the Canadian Foundation for Innovation (CFI), Canadian Institutes of Health Research (CIHR), and Terry Fox Research Institute (TFRI). We acknowledge salary support from the McGill Integrated Cancer Research Training Program (to E.H.M. and S.I.), the Cole Foundation (to S.I.), the Fonds de la Recherche du Québec – Santé (FRQS, to E.H.M., S.I., and T.F.D.), and the CIHR (to R.G.J.). This research has been supported by grants from the CIHR (MOP-136915 to S.M.S., MOP-123352 to T.F.D., and MOP-93799 to R.G.J.) and Terry Fox Research Institute (TFRI-239585 to R.G.J.). This work is dedicated to the memory of Rosalind Goodman.

Received: March 30, 2016
Revised: June 2, 2016
Accepted: July 14, 2016
Published: August 4, 2016

REFERENCES

Agarwal, V., Bell, G.W., Nam, J.W., and Bartel, D.P. (2015). Predicting effective microRNA target sites in mammalian mRNAs. eLife *4*, 4.

Barrans, S., Crouch, S., Smith, A., Turner, K., Owen, R., Patmore, R., Roman, E., and Jack, A. (2010). Rearrangement of MYC is associated with poor prognosis in patients with diffuse large B-cell lymphoma treated in the era of rituximab. J. Clin. Oncol. *28*, 3360–3365.

Bartel, D.P. (2009). MicroRNAs: target recognition and regulatory functions. Cell *136*, 215–233.

Birsoy, K., Wang, T., Chen, W.W., Freinkman, E., Abu-Remaileh, M., and Sabatini, D.M. (2015). An essential role of the mitochondrial electron transport chain in cell proliferation is to enable aspartate synthesis. Cell *162*, 540–551.

Bott, A.J., Peng, I.C., Fan, Y., Faubert, B., Zhao, L., Li, J., Neidler, S., Sun, Y., Jaber, N., Krokowski, D., et al. (2015). Oncogenic Myc induces expression of glutamine synthetase through promoter demethylation. Cell Metab. *22*, 1068–1077.

Bredel, M., Scholtens, D.M., Harsh, G.R., Bredel, C., Chandler, J.P., Renfrow, J.J., Yadav, A.K., Vogel, H., Scheck, A.C., Tibshirani, R., and Sikic, B.I. (2009). A network model of a cooperative genetic landscape in brain tumors. JAMA *302*, 261–275.

Cancer Genome Atlas Network (2012). Comprehensive molecular characterization of human colon and rectal cancer. Nature *487*, 330–337.

Cancer Genome Atlas Research Network (2014). Comprehensive molecular profiling of lung adenocarcinoma. Nature *511*, 543–550.

Cerami, E., Gao, J., Dogrusoz, U., Gross, B.E., Sumer, S.O., Aksoy, B.A., Jacobsen, A., Byrne, C.J., Heuer, M.L., Larsson, E., et al. (2012). The cBio cancer genomics portal: an open platform for exploring multidimensional cancer genomics data. Cancer Discov. *2*, 401–404.

Chang, T.C., Yu, D., Lee, Y.S., Wentzel, E.A., Arking, D.E., West, K.M., Dang, C.V., Thomas-Tikhonenko, A., and Mendell, J.T. (2008). Widespread microRNA repression by Myc contributes to tumorigenesis. Nat. Genet. *40*, 43–50.

Conkrite, K., Sundby, M., Mukai, S., Thomson, J.M., Mu, D., Hammond, S.M., and MacPherson, D. (2011). miR-17∼92 cooperates with RB pathway mutations to promote retinoblastoma. Genes Dev. *25*, 1734–1745.

Dang, C.V. (2012). MYC on the path to cancer. Cell *149*, 22–35.

Deberardinis, R.J., Sayed, N., Ditsworth, D., and Thompson, C.B. (2008). Brick by brick: metabolism and tumor cell growth. Curr. Opin. Genet. Dev. *18*, 54–61.

Dews, M., Homayouni, A., Yu, D., Murphy, D., Sevignani, C., Wentzel, E., Furth, E.E., Lee, W.M., Enders, G.H., Mendell, J.T., and Thomas-Tikhonenko, A. (2006). Augmentation of tumor angiogenesis by a Myc-activated microRNA cluster. Nat. Genet. *38*, 1060–1065.

Du, P., Wang, L., Sliz, P., and Gregory, R.I. (2015). A biogenesis step upstream of microprocessor controls miR-17∼92 expression. Cell *162*, 885–899.

Dupuy, F., Griss, T., Blagih, J., Bridon, G., Avizonis, D., Ling, C., Dong, Z., Siwak, D.R., Annis, M.G., Mills, G.B., et al. (2013). LKB1 is a central regulator of tumor initiation and pro-growth metabolism in ErbB2-mediated breast cancer. Cancer Metab. *1*, 18.

Fabian, M.R., Sonenberg, N., and Filipowicz, W. (2010). Regulation of mRNA translation and stability by microRNAs. Annu. Rev. Biochem. *79*, 351–379.

Faubert, B., Boily, G., Izreig, S., Griss, T., Samborska, B., Dong, Z., Dupuy, F., Chambers, C., Fuerth, B.J., Viollet, B., et al. (2013). AMPK is a negative regulator of the Warburg effect and suppresses tumor growth in vivo. Cell Metab. *17*, 113–124.

Faubert, B., Vincent, E.E., Griss, T., Samborska, B., Izreig, S., Svensson, R.U., Mamer, O.A., Avizonis, D., Shackelford, D.B., Shaw, R.J., and Jones, R.G.

(2014). Loss of the tumor suppressor LKB1 promotes metabolic reprogramming of cancer cells via HIF-1α. Proc. Natl. Acad. Sci. USA *111*, 2554–2559.

Gao, P., Tchernyshyov, I., Chang, T.C., Lee, Y.S., Kita, K., Ochi, T., Zeller, K.I., De Marzo, A.M., Van Eyk, J.E., Mendell, J.T., and Dang, C.V. (2009). c-Myc suppression of miR-23a/b enhances mitochondrial glutaminase expression and glutamine metabolism. Nature *458*, 762–765.

Gill, R.K., Yang, S.H., Meerzaman, D., Mechanic, L.E., Bowman, E.D., Jeon, H.S., Roy Chowdhuri, S., Shakoori, A., Dracheva, T., Hong, K.M., et al. (2011). Frequent homozygous deletion of the LKB1/STK11 gene in non-small cell lung cancer. Oncogene *30*, 3784–3791.

Godlewski, J., Nowicki, M.O., Bronisz, A., Nuovo, G., Palatini, J., De Lay, M., Van Brocklyn, J., Ostrowski, M.C., Chiocca, E.A., and Lawler, S.E. (2010). MicroRNA-451 regulates LKB1/AMPK signaling and allows adaptation to metabolic stress in glioma cells. Mol. Cell *37*, 620–632.

Hamlyn, P.H., and Rabbitts, T.H. (1983). Translocation joins c-myc and immunoglobulin gamma 1 genes in a Burkitt lymphoma revealing a third exon in the c-myc oncogene. Nature *304*, 135–139.

Hatzivassiliou, G., Zhao, F., Bauer, D.E., Andreadis, C., Shaw, A.N., Dhanak, D., Hingorani, S.R., Tuveson, D.A., and Thompson, C.B. (2005). ATP citrate lyase inhibition can suppress tumor cell growth. Cancer Cell *8*, 311–321.

Hayashita, Y., Osada, H., Tatematsu, Y., Yamada, H., Yanagisawa, K., Tomida, S., Yatabe, Y., Kawahara, K., Sekido, Y., and Takahashi, T. (2005). A polycistronic microRNA cluster, miR-17-92, is overexpressed in human lung cancers and enhances cell proliferation. Cancer Res. *65*, 9628–9632.

He, L., Thomson, J.M., Hemann, M.T., Hernando-Monge, E., Mu, D., Goodson, S., Powers, S., Cordon-Cardo, C., Lowe, S.W., Hannon, G.J., and Hammond, S.M. (2005). A microRNA polycistron as a potential human oncogene. Nature *435*, 828–833.

Helwak, A., Kudla, G., Dudnakova, T., and Tollervey, D. (2013). Mapping the human miRNA interactome by CLASH reveals frequent noncanonical binding. Cell *153*, 654–665.

Hong, L., Lai, M., Chen, M., Xie, C., Liao, R., Kang, Y.J., Xiao, C., Hu, W.Y., Han, J., and Sun, P. (2010). The miR-17-92 cluster of microRNAs confers tumorigenicity by inhibiting oncogene-induced senescence. Cancer Res. *70*, 8547–8557.

Jha, A.K., Huang, S.C., Sergushichev, A., Lampropoulou, V., Ivanova, Y., Loginicheva, E., Chmielewski, K., Stewart, K.M., Ashall, J., Everts, B., et al. (2015). Network integration of parallel metabolic and transcriptional data reveals metabolic modules that regulate macrophage polarization. Immunity *42*, 419–430.

Jones, R.G., and Thompson, C.B. (2009). Tumor suppressors and cell metabolism: a recipe for cancer growth. Genes Dev. *23*, 537–548.

Kim, J., Woo, A.J., Chu, J., Snow, J.W., Fujiwara, Y., Kim, C.G., Cantor, A.B., and Orkin, S.H. (2010). A Myc network accounts for similarities between embryonic stem and cancer cell transcription programs. Cell *143*, 313–324.

Knudsen, K.N., Nielsen, B.S., Lindebjerg, J., Hansen, T.F., Holst, R., and Sørensen, F.B. (2015). microRNA-17 is the most up-regulated member of the miR-17-92 cluster during early colon cancer evolution. PLoS ONE *10*, e0140503.

Landais, S., Landry, S., Legault, P., and Rassart, E. (2007). Oncogenic potential of the miR-106-363 cluster and its implication in human T-cell leukemia. Cancer Res. *67*, 5699–5707.

Le, A., Lane, A.N., Hamaker, M., Bose, S., Gouw, A., Barbi, J., Tsukamoto, T., Rojas, C.J., Slusher, B.S., Zhang, H., et al. (2012). Glucose-independent glutamine metabolism via TCA cycling for proliferation and survival in B cells. Cell Metab. *15*, 110–121.

Li, Q., Seo, J.H., Stranger, B., McKenna, A., Pe'er, I., Laframboise, T., Brown, M., Tyekucheva, S., and Freedman, M.L. (2013). Integrative eQTL-based analyses reveal the biology of breast cancer risk loci. Cell *152*, 633–641.

Li, Y., Choi, P.S., Casey, S.C., Dill, D.L., and Felsher, D.W. (2014). MYC through miR-17-92 suppresses specific target genes to maintain survival, autonomous proliferation, and a neoplastic state. Cancer Cell *26*, 262–272.

Lin, C.Y., Lovén, J., Rahl, P.B., Paranal, R.M., Burge, C.B., Bradner, J.E., Lee, T.I., and Young, R.A. (2012a). Transcriptional amplification in tumor cells with elevated c-Myc. Cell *151*, 56–67.

Lin, P., Dickason, T.J., Fayad, L.E., Lennon, P.A., Hu, P., Garcia, M., Routbort, M.J., Miranda, R., Wang, X., Qiao, W., and Medeiros, L.J. (2012b). Prognostic value of MYC rearrangement in cases of B-cell lymphoma, unclassifiable, with features intermediate between diffuse large B-cell lymphoma and Burkitt lymphoma. Cancer *118*, 1566–1573.

Liu, T., Qin, W., Hou, L., and Huang, Y. (2015). MicroRNA-17 promotes normal ovarian cancer cells to cancer stem cells development via suppression of the LKB1-p53-p21/WAF1 pathway. Tumour Biol. *36*, 1881–1893.

Lunt, S.Y., and Vander Heiden, M.G. (2011). Aerobic glycolysis: meeting the metabolic requirements of cell proliferation. Annu. Rev. Cell Dev. Biol. *27*, 441–464.

Luo, W., Friedman, M.S., Shedden, K., Hankenson, K.D., and Woolf, P.J. (2009). GAGE: generally applicable gene set enrichment for pathway analysis. BMC Bioinformatics *10*, 161.

McGuirk, S., Gravel, S.P., Deblois, G., Papadopoli, D.J., Faubert, B., Wegner, A., Hiller, K., Avizonis, D., Akavia, U.D., Jones, R.G., et al. (2013). PGC-1α supports glutamine metabolism in breast cancer. Cancer Metab. *1*, 22.

Mu, P., Han, Y.C., Betel, D., Yao, E., Squatrito, M., Ogrodowski, P., de Stanchina, E., D'Andrea, A., Sander, C., and Ventura, A. (2009). Genetic dissection of the miR-17∼92 cluster of microRNAs in Myc-induced B-cell lymphomas. Genes Dev. *23*, 2806–2811.

Nie, Z., Hu, G., Wei, G., Cui, K., Yamane, A., Resch, W., Wang, R., Green, D.R., Tessarollo, L., Casellas, R., et al. (2012). c-Myc is a universal amplifier of expressed genes in lymphocytes and embryonic stem cells. Cell *151*, 68–79.

O'Donnell, K.A., Wentzel, E.A., Zeller, K.I., Dang, C.V., and Mendell, J.T. (2005). c-Myc-regulated microRNAs modulate E2F1 expression. Nature *435*, 839–843.

Olive, V., Bennett, M.J., Walker, J.C., Ma, C., Jiang, I., Cordon-Cardo, C., Li, Q.J., Lowe, S.W., Hannon, G.J., and He, L. (2009). miR-19 is a key oncogenic component of mir-17-92. Genes Dev. *23*, 2839–2849.

Olive, V., Jiang, I., and He, L. (2010). mir-17-92, a cluster of miRNAs in the midst of the cancer network. Int. J. Biochem. Cell Biol. *42*, 1348–1354.

Olive, V., Li, Q., and He, L. (2013). mir-17-92: a polycistronic oncomir with pleiotropic functions. Immunol. Rev. *253*, 158–166.

Ota, A., Tagawa, H., Karnan, S., Tsuzuki, S., Karpas, A., Kira, S., Yoshida, Y., and Seto, M. (2004). Identification and characterization of a novel gene, C13orf25, as a target for 13q31-q32 amplification in malignant lymphoma. Cancer Res. *64*, 3087–3095.

Pei, H., Ma, N., Chen, J., Zheng, Y., Tian, J., Li, J., Zhang, S., Fei, Z., and Gao, J. (2013). Integrative analysis of miRNA and mRNA profiles in response to ethylene in rose petals during flower opening. PLoS ONE *8*, e64290.

Savage, K.J., Johnson, N.A., Ben-Neriah, S., Connors, J.M., Sehn, L.H., Farinha, P., Horsman, D.E., and Gascoyne, R.D. (2009). MYC gene rearrangements are associated with a poor prognosis in diffuse large B-cell lymphoma patients treated with R-CHOP chemotherapy. Blood *114*, 3533–3537.

Schmitz, R., Young, R.M., Ceribelli, M., Jhavar, S., Xiao, W., Zhang, M., Wright, G., Shaffer, A.L., Hodson, D.J., Buras, E., et al. (2012). Burkitt lymphoma pathogenesis and therapeutic targets from structural and functional genomics. Nature *490*, 116–120.

Shackelford, D.B., and Shaw, R.J. (2009). The LKB1-AMPK pathway: metabolism and growth control in tumour suppression. Nat. Rev. Cancer *9*, 563–575.

Shackelford, D.B., Vasquez, D.S., Corbeil, J., Wu, S., Leblanc, M., Wu, C.L., Vera, D.R., and Shaw, R.J. (2009). mTOR and HIF-1alpha-mediated tumor metabolism in an LKB1 mouse model of Peutz-Jeghers syndrome. Proc. Natl. Acad. Sci. USA *106*, 11137–11142.

Shaw, R.J., Bardeesy, N., Manning, B.D., Lopez, L., Kosmatka, M., DePinho, R.A., and Cantley, L.C. (2004). The LKB1 tumor suppressor negatively regulates mTOR signaling. Cancer Cell *6*, 91–99.

Smith, D.P., Spicer, J., Smith, A., Swift, S., and Ashworth, A. (1999). The mouse Peutz-Jeghers syndrome gene Lkb1 encodes a nuclear protein kinase. Hum. Mol. Genet. *8*, 1479–1485.

Stine, Z.E., Walton, Z.E., Altman, B.J., Hsieh, A.L., and Dang, C.V. (2015). MYC, Metabolism, and Cancer. Cancer Discov. *5*, 1024–1039.

Sullivan, L.B., Gui, D.Y., Hosios, A.M., Bush, L.N., Freinkman, E., and Vander Heiden, M.G. (2015). Supporting aspartate biosynthesis is an essential function of respiration in proliferating cells. Cell *162*, 552–563.

Vaahtomeri, K., and Mäkelä, T.P. (2011). Molecular mechanisms of tumor suppression by LKB1. FEBS Lett. *585*, 944–951.

Valdmanis, P.N., Gu, S., Schüermann, N., Sethupathy, P., Grimm, D., and Kay, M.A. (2012). Expression determinants of mammalian argonaute proteins in mediating gene silencing. Nucleic Acids Res. *40*, 3704–3713.

Vander Heiden, M.G., Cantley, L.C., and Thompson, C.B. (2009). Understanding the Warburg effect: the metabolic requirements of cell proliferation. Science *324*, 1029–1033.

Vincent, E.E., Coelho, P.P., Blagih, J., Griss, T., Viollet, B., and Jones, R.G. (2015a). Differential effects of AMPK agonists on cell growth and metabolism. Oncogene *34*, 3627–3639.

Vincent, E.E., Sergushichev, A., Griss, T., Gingras, M.C., Samborska, B., Ntimbane, T., Coelho, P.P., Blagih, J., Raissi, T.C., Choinière, L., et al. (2015b). Mitochondrial phosphoenolpyruvate carboxykinase regulates metabolic adaptation and enables glucose-independent tumor growth. Mol. Cell *60*, 195–207.

Wang, R., Dillon, C.P., Shi, L.Z., Milasta, S., Carter, R., Finkelstein, D., McCormick, L.L., Fitzgerald, P., Chi, H., Munger, J., and Green, D.R. (2011). The transcription factor Myc controls metabolic reprogramming upon T lymphocyte activation. Immunity *35*, 871–882.

Weinberg, S.E., and Chandel, N.S. (2015). Targeting mitochondria metabolism for cancer therapy. Nat. Chem. Biol. *11*, 9–15.

Wise, D.R., DeBerardinis, R.J., Mancuso, A., Sayed, N., Zhang, X.Y., Pfeiffer, H.K., Nissim, I., Daikhin, E., Yudkoff, M., McMahon, S.B., and Thompson, C.B. (2008). Myc regulates a transcriptional program that stimulates mitochondrial glutaminolysis and leads to glutamine addiction. Proc. Natl. Acad. Sci. USA *105*, 18782–18787.

Wolf, E., Lin, C.Y., Eilers, M., and Levens, D.L. (2015). Taming of the beast: shaping Myc-dependent amplification. Trends Cell Biol. *25*, 241–248.

Wu, M., Neilson, A., Swift, A.L., Moran, R., Tamagnine, J., Parslow, D., Armistead, S., Lemire, K., Orrell, J., Teich, J., et al. (2007). Multiparameter metabolic analysis reveals a close link between attenuated mitochondrial bioenergetic function and enhanced glycolysis dependency in human tumor cells. Am. J. Physiol. Cell Physiol. *292*, C125–C136.

Wu, E., Thivierge, C., Flamand, M., Mathonnet, G., Vashisht, A.A., Wohlschlegel, J., Fabian, M.R., Sonenberg, N., and Duchaine, T.F. (2010). Pervasive and cooperative deadenylation of 3'UTRs by embryonic microRNA families. Mol. Cell *40*, 558–570.

Yoo, L.I., Chung, D.C., and Yuan, J. (2002). LKB1–a master tumour suppressor of the small intestine and beyond. Nat. Rev. Cancer *2*, 529–535.

Yu, J., Ohuchida, K., Mizumoto, K., Fujita, H., Nakata, K., and Tanaka, M. (2010). MicroRNA miR-17-5p is overexpressed in pancreatic cancer, associated with a poor prognosis, and involved in cancer cell proliferation and invasion. Cancer Biol. Ther. *10*, 748–757.

Zack, T.I., Schumacher, S.E., Carter, S.L., Cherniack, A.D., Saksena, G., Tabak, B., Lawrence, M.S., Zhsng, C.Z., Wala, J., Mermel, C.H., et al. (2013). Pan-cancer patterns of somatic copy number alteration. Nat. Genet. *45*, 1134–1140.

Zhou, M., Wang, J., Ouyang, J., Xu, J.Y., Chen, B., Zhang, Q.G., Zhou, R.F., Yang, Y.G., Shao, X.Y., Xu, Y., et al. (2014). MYC protein expression is associated with poor prognosis in diffuse large B cell lymphoma patients treated with RCHOP chemotherapy. Tumour Biol. *35*, 6757–6762.